

Shear-dependent morphology of von Willebrand factor bound to immobilized collagen

Levente Novák, Hans Deckmyn, Sándor Damjanovich, and Jolán Hársfalvi

We have developed an immunogold von Willebrand factor (VWF) detection method that permits almost complete coverage of individual VWF molecules, and by this unequivocal localization and morphologic analysis of collagen-bound VWF by atomic force microscopy (AFM). Perfusion of gel filtration-purified VWF in parallel plate perfusion chambers over glass coverslips coated with calf skin collagen, followed by AFM imaging in air, enabled us to assess possible morphologic differences between VWF bound at low ($0.07 \text{ N/m}^2 = 0.7 \text{ dynes/cm}^2$) and high ($4.55 \text{ N/m}^2 = 45.5 \text{ dynes/cm}^2$) shear stresses. No significant differences in VWF morphology were found, the molecules were oriented almost randomly, and there were no clear signs of VWF "uncoiling" either at a high or at a low shear regime. After perfusing $1 \mu\text{g/mL}$ VWF for 5 minutes, surface coverage at high shear was almost twice the one seen at low shear, and some larger and more irregularly shaped VWF molecules could be seen at high shear. This difference disappeared, however, at 15 minutes of perfusion and was probably caused by diffusion kinetics. Moreover, the presence of

$68 \times 10^9/\text{L}$ washed fixed platelets in the perfusate did not have any visible effect on VWF morphology at high versus low shear stress. These findings suggest that shear stress does not influence significantly the overall molecular morphology of VWF during its binding to collagen-coated surface and are consistent with a constitutively expressed affinity of collagen-bound VWF for glycoprotein Ib. (Blood. 2002;99:2070-2076)

© 2002 by The American Society of Hematology

Introduction

von Willebrand factor (VWF) is a multimeric glycoprotein required for platelet adhesion at sites of high wall shear stress. Although its hemostatic properties are thoroughly investigated and the binding sites to glycoprotein Ib (GPIb), glycoprotein IIb-IIIa (GPIIb-IIIa), factor VIII, collagen, and heparin determined, little is known about the mechanisms of its ability to promote platelet tethering and arrest at wound sites.¹

VWF monomers (protomers) have a trinodular structure resembling the one of fibrinogen but with quite different molecular dimensions.² The approximately 120-nm long protomer is composed of 2 globular domains joined by 2 rodlike domains and a central globular nodule. Protomers assemble to multimers of variable polymerization degree (from 2 to more than 40 protomers/multimer) that can possess different shapes in solution. Most often, they are observed as having a coiled structure with a size of about 100 to 300 nm, but sometimes extended, uncoiled forms are also apparent in some preparations.²

VWF in solution does not bind to nonstimulated healthy platelets in the absence of modulators. However, platelets adhere to VWF bound to several types of adhesive proteins, and the extent of this interaction depends on the shear rate. At high shear rates, platelet tethering depends mostly on VWF-GPIb interaction.³ Additionally, a very large shear stress can induce VWF-dependent platelet aggregation even in the absence of adhesive proteins.⁴

These observations indicate that shear plays an important role in the interaction between VWF and GPIb.

It is not clear whether VWF undergoes a conformational change on binding to subendothelium or to collagen under high shear stress, or whether it is equally active at low and high shear with a very rapid association-dissociation rate to platelet GPIb and, thus, requires no conformational change to be fully active.³ This latter type of interaction would first considerably decrease the linear velocity of platelets, which then could afterward firmly fix themselves to VWF through their GPIIb-IIIa receptors.^{3,5} A previous atomic force microscopy (AFM) study, using VWF dynamically adsorbed onto octadecyl-trichlorosilane-treated glass, indicated that VWF can uncoil at shear stresses above 3.5 N/m^2 (35 dynes/cm^2).⁶

To investigate the possible effects of shear stress on the submicroscopic morphology of VWF, we performed dynamic binding experiments to glass coverslips coated with calf skin collagen type I in parallel-plate perfusion chambers. Specific gold-coupled antibody labeling was necessary to unequivocally identify VWF adsorbed to calf skin collagen by AFM. Image analysis of AFM pictures allowed us to quantify morphologic parameters of VWF. No significant differences were found in respect to the molecular morphology or the orientation of VWF molecules bound to collagen at low ($0.07 \text{ N/m}^2 = 0.7 \text{ dynes/cm}^2$) or high ($4.55 \text{ N/m}^2 = 45.5 \text{ dynes/cm}^2$) shear stress.

From the University of Debrecen, Medical and Health Science Center, Department of Clinical Biochemistry and Molecular Pathology, and the Department of Biophysics and Cell Biology, Debrecen, Hungary; and the Catholic University of Leuven, Campus Kortrijk, Interdisciplinary Research Center, Kortrijk, Belgium.

Submitted August 31, 2001; accepted November 13, 2001.

Supported by OMFB Tét B-13/96; BIOMED ERBMC20C980207; and OTKA T 022520.

Reprints: Jolán Hársfalvi, University of Debrecen, Medical and Health Science Center, Department of Clinical Biochemistry and Molecular Pathology, PO Box 40, Debrecen, H-4012, Hungary; e-mail: harsfalv@jaguar.dote.hu.

The publication costs of this article were defrayed in part by page charge payment. Therefore, and solely to indicate this fact, this article is hereby marked "advertisement" in accordance with 18 U.S.C. section 1734.

© 2002 by The American Society of Hematology

Materials and methods

Preparation of protein A–gold conjugates

Gold sol was prepared by citrate reduction of gold chloride.⁷ To 50 mL distilled water, 1 mL 1% gold chloride hydrate (containing approximately 49% gold; Fluka, Buchs, Switzerland) was added, the solution brought to boil, then 0.75 mL 1% trisodium citrate 2 H₂O was rapidly mixed into the stirred mixture and refluxed until the color turned to red. This sol, consisting of approximately 30-nm diameter particles, was then cooled down and titrated to pH = 6.5 with 0.2 M potassium carbonate solution. Gold particles of about 15 nm were synthesized by adding a higher amount (4 mL) of trisodium citrate into the boiling gold chloride solution.

To determine the quantity of protein A required to stabilize the gold solution, 100 μ L sol was mixed with increasing amounts of protein A (Pharmacia, Uppsala, Sweden) dissolved in distilled water. After 5 minutes, 11 μ L of 10 times concentrated phosphate buffered saline (10 \times PBS, containing 1.45 M NaCl and 0.2 M sodium phosphate at pH = 7.35) was added to the vials, and the color change was evaluated after 30 minutes of standing. Usually, 2 to 3 μ g protein A/mL gold sol was sufficient to stabilize the particles against salt-induced flocculation. To fully saturate gold beads with protein, we routinely added 6 μ g protein A to 1 mL sol, then aqueous Tween 20 was mixed into the solution at a final concentration of 0.02% to further stabilize the complex.

Protein A–gold was centrifuged at 10°C in 1.5-mL polypropylene microcentrifuge tubes (at 7500g for 11 minutes in the case of 30-nm particles, and 10 000g for 25 minutes for 15-nm gold), then most of the supernatant was carefully removed, and the pellet was resuspended in the remainder. The concentrated conjugate was applied onto a 25 \times 5-cm BioGel A 5m-column (BioRad, Hercules, CA) and eluted with PBS containing 0.02% Tween 20 and 0.02% NaN₃ in 1.5-mL fractions. The second, third, and fourth gold-containing (reddish) fractions were saved and pooled together, and the other fractions were discarded. This procedure resulted in a monodisperse sol free of aggregates. The conjugate solution was stored at 4°C, with no signs of deterioration even after 4 months.

VWF purification and analysis

VWF was purified from commercial VWF:FVIII concentrate (Haemate P; Centeon Pharma GmbH, Austria) by gel filtration. Haemate P (2.5 mL) at a concentration of 500 μ g/mL VWF was applied to a 90 \times 1.4-cm Sepharose CL-4B (Pharmacia AB, Uppsala, Sweden) column equilibrated in PBS and eluted at a flow rate of 0.5 mL/minute into 2.5-mL fractions. The protein content of the fractions was assayed by bicinchoninic acid reagent (Pierce, Rockford, IL). VWF eluted near the column void volume. These fractions contained only VWF as determined by sodium dodecyl sulfate–polyacrylamide gel electrophoresis (SDS-PAGE) under reducing conditions. Generally, the first 2 fractions containing only larger multimers were used for the experiments.

To determine the multimeric distribution of the VWF fractions, a 1.7% agarose-SDS gel electrophoresis was performed in parallel with unpurified Haemate P and human platelet-poor plasma (mixed control from 5 healthy donors). The proteins were blotted onto polyvinylidene difluoride membrane with a Bio-Rad (Hercules, CA) Trans-Blot SD semidry blotting apparatus. The membrane was blocked with 0.5% casein in PBS for 1 hour, then VWF was detected with peroxidase-labeled rabbit antihuman VWF polyclonal antibody (DAKO, Glostrup, Denmark) and 3,3'-diaminobenzidine. Multimeric analysis revealed that unpurified Haemate-P contains small as well as large multimers, ranging from dimers to at least 22-mers, whereas the first purified fractions collected were devoid of the smaller multimers.

Coverslip preparation

Rectangular 18 \times 24-mm glass coverslips were used as AFM support, of which the upper left corner was cut down to avoid possible confusion between collagen-coated and uncoated surfaces during subsequent manipu-

lation steps. Coverslips were soaked in methanol, wiped with paper tissue, then heated for 45 seconds over a Bunsen flame.

Surface coating with collagen was performed by placing the coverslips for 2 hours onto 50- μ L drops of 1 mg/mL calf skin collagen type I (Sigma type III; Sigma-Aldrich Kft, Budapest, Hungary) dissolved in 50 mM acetic acid. Subsequently, all coated and noncoated coverslips were washed in PBS (containing 145 mM NaCl and 20 mM sodium phosphate at pH = 7.35) for at least 30 minutes and kept in this buffer until shear experiments.

Shear experiments, binding of VWF onto collagen

Controlled shear rate experiments were performed in parallel plate perfusion chambers,⁸ which accommodate 18 \times 24-mm coverslips. Coated or noncoated coverslips were then placed into the chamber and perfused with PBS containing 1 μ g/mL VWF. Perfusion continued for 5 or 15 minutes at 37°C with 100/s or 6500/s shear rate, corresponding to approximately 0.07 N/m² and approximately 4.55 N/m² shear stress, respectively. For each condition, appropriate blanks were run with PBS instead of VWF solution.

After perfusion, coverslips were rinsed in situ with at least 15 mL fresh PBS, then fixed with 2% paraformaldehyde in PBS for 3 minutes in flow and additionally for 12 minutes out of flow. After the fixation, free aldehyde groups that could remain on the fixed proteins were quenched for at least 15 minutes in 0.1 M ammonium sulfate + 25 mM sodium phosphate buffer (pH = 7.4).

VWF detection

Coverslips were subsequently washed with PBS and blocked in PBS containing 0.5% bovine casein ("casein acc. to Hammarsten"; Merck KGaA, Darmstadt, Germany) and 0.05% Tween 20 for 30 minutes (the solution was centrifuged at 23 100g for 20 minutes before use to remove possible protein aggregates), then 1 mL/coverslip anti-VWF antibody (DAKO) diluted 1/500 in PBS + 0.05% Tween 20 (PBS-T) was applied overnight at 4°C. Samples were then soaked 4 times in PBS-T, followed by 2 hours' incubation in either protein A coupled to 15-nm gold markers, or successively in protein A 30-nm gold, then in protein A 15-nm gold conjugate (double labeling). On some samples, the red color of deposited gold complex was clearly visible by the end of this time. Coverslips were then rinsed several times with PBS-T, the gold probes fixed onto the VWF with 2% paraformaldehyde in PBS for 60 minutes, and, finally, the samples were thoroughly rinsed in distilled water and dried in air.

AFM imaging

The instrument used was assembled at the Institute of Biophysics and Cell Biology (University of Debrecen, Hungary) from parts purchased from the University of Twente (Enschede, The Netherlands). The piezoelectric scanner drives directly the cantilever instead of the sample, thus making possible the use of conventional glass microscopic slides mounted on a Zeiss Axiophot inverted microscope. Coverslips were glued onto glass slides with cyanoacrylate adhesive and imaged in air with Microlever-sharpened silicon nitride tips (Park Scientific, Sunnyvale, CA) having nominally 20-nm radius of curvature, or Ultralever high-aspect ratio silicon tips (approximately 10 nm of radius). Usually intermittent-contact mode was used with "F"-type microlevers or "D"-type ultralevers at a few tenths of a kilohertz below their resonant frequency (around 120 kHz and 160 kHz, respectively). Contact-mode imaging was only successful at very low ambient relative humidities, as tips regularly stuck to the sample when this latter was covered by a thin layer of adsorbed water. We collected 512 \times 512 pixel images with scan speeds of 0.7 to 1.5 lines/second, simultaneously in height and error signal modes. The scanned images were not corrected for tip convolution, but all samples from a given experiment were measured the same day without changing the tip, ensuring comparability between images.

Image analysis

Images (4–8.5 \times 5 μ m²) were taken from the shear area of each coverslip, and morphologic analysis was performed with the publicly available free software UTHSCSA ImageTool (developed at the University of Texas

Health Science Center at San Antonio, TX, and available from the Internet at <http://ddsdx.uthscsa.edu/>). Height field and reconstructed images were produced with the free software *gxsm* (<http://gxsm.sourceforge.net/>), *gnuplot* (<http://www.gnuplot.org/>), and *Image/J* (<http://rsb.info.nih.gov/ij/>).

First, AFM-acquired images were binarized by thresholding to include only the gold particle-covered area. Background removal was then performed on each image to filter off nonspecifically bound gold beads: a maximal cut-off size was defined to exclude all singlets, then the (very few) background doublets were removed manually.

The remaining "islands," consisting of VWF molecules covered by immunogold, were subjected to morphologic analysis, in respect to the following parameters: area (A), perimeter length (P), major (x) and minor axis length (y) of the best-fit ellipse, major (α) and minor axis angle (β) toward the flow direction, eccentricity ($E = x/y$), roundness ($R = 4\pi A/P^2$), feret diameter ($F = 2 \times (A/\pi)^{1/2}$) (corresponding to the diameter of a circle having the same area as the measured particle; a more detailed explanation of these morphological parameters can be found in *ImageTool's* manual, freely available on the Internet at <http://ddsdx.uthscsa.edu/>), as well as the percentage of surface coverage ($C\%$). Of these parameters, E and R are particularly useful in determining whether VWF molecules are oblong and/or lobulated, whereas the scatter in α and β values indicate how evenly oriented the individual molecules are. To compare the effect of low and high shear experimental conditions on overall VWF morphology, arithmetic mean and SD values were calculated from most parameters.

Platelet washing and fixation

Citrated blood from 20 donors was centrifuged at 150g for 15 minutes to prepare platelet-rich plasma. Platelets were washed 3 times with buffer containing 20 mM Tris, 1 mM EDTA- Na_2 , 146 mM NaCl, and 5 mM glucose, then fixed in 2% paraformaldehyde dissolved in PBS overnight at 4°C. After fixation, platelets were washed 4 times and resuspended in PBS containing 0.02% NaN_3 .

Results

Adsorption of VWF onto glass and collagen

Initially, we thought that purification of our VWF preparation (Haemate P) is not necessary, as a specific labeling method will be used to detect VWF. Contrary to what we expected, VWF from this concentrate—that contains several proteins as determined by reducing SDS-PAGE gel—sticks well to bare glass and adheres to a lesser extent to calf skin collagen-coated coverslips. Blocking the coverslips either with bovine serum albumin or 0.05% to 0.1% Tween-20 did not reduce the nonspecific adhesion, but rather seemed to enhance it. In consequence, the raw VWF preparation was freed from human serum albumin and other contaminant proteins by gel filtration, and VWF was diluted with unsupplemented PBS during all subsequent experiments.

It is technically difficult to test the functionality of collagen-bound VWF toward GPIb because of the direct interactions between collagen and the platelet collagen receptors, but as the purified VWF was active in the ristocetin-induced platelet aggregation test and it is known that binding to collagen does not abolish the functionality of VWF toward GPIb, it is reasonable to assume that our collagen-bound VWF retained its capacity to mediate shear-dependent platelet adhesion.⁹

Labeling efficiency of VWF

The use of blocking agents to diminish unspecific background binding of immunogold is widely used in electron microscopy. These molecules can, however, interfere with sample topography in AFM. To overcome this problem, some researchers avoid blocking at all and use highly diluted antibodies, at the expense of a low labeling efficiency.¹⁰ In our case, it was imperative to obtain high

label yields while maintaining background binding as low as possible. Therefore, we decided to use a blocking agent having a small molecule size. Originally, blocking before immunodetection was performed with 0.1% Tween 20 in PBS, but this procedure yielded a relatively high background. Experimenting with VWF blotted onto nitrocellulose membrane showed that the best blocking reagents were 0.5% bovine casein in PBS and 0.05% Tween 80 in PBS, with, however, a very clear preference toward casein. This latter, chosen for all subsequent experiments, did not interfere with the AFM measures.

At the dilutions used (1/10× in PBS + 0.05% Tween 20), gold-coupled protein A labeled very efficiently the VWF-anti-VWF complex; individual molecules were completely covered up by gold beads (Figure 1A,B). As expected, background binding was also relatively high but could always be completely discriminated from specific labeling, as nonspecifically stuck gold particles were almost exclusively singlets with a very low percentage of doublets and virtually no larger aggregates (Figure 1C).

During the first experiments, double labeling with 30-nm and 15-nm gold particles was performed on the samples to ascertain that gold markers are indeed visible on the collagen-coated surface. Larger gold spheres can be located easily, but they do not cover the VWF molecules densely enough to be really useable for morphologic purposes. However, it was not certain whether smaller particles could be easily distinguished on the rough background. Finally, we have found that 15-nm gold-coupled antibodies can be successfully used.

In each experiment, integrity of the collagen coating was carefully checked and was found to form always a continuous monolayer (Figure 1C) covering uniformly the surface and was

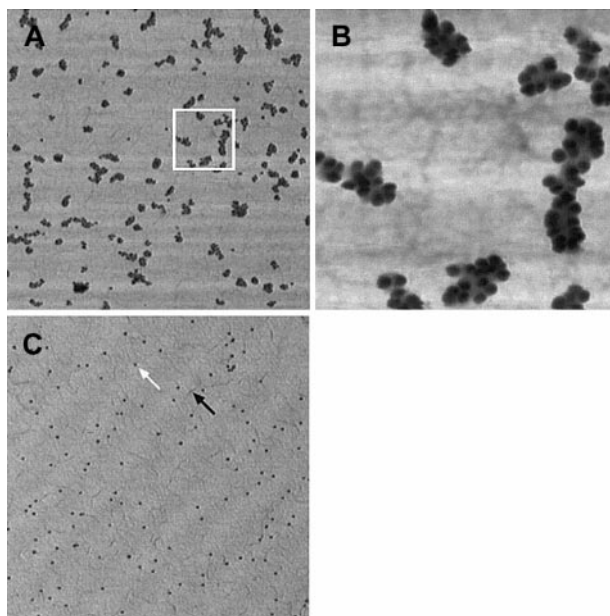


Figure 1. VWF labeling efficiency and specificity by immunogold method. (A) Individual VWF molecules are almost completely covered by gold spheres. VWF bound to collagen was visualized by polyclonal anti-VWF antibody treatment, followed by protein-A-conjugated gold (15-nm diameter beads). (B) Magnified detail of the area delimited by a white square. (C) Nonspecific binding of immunogold on collagen. PBS-perfused collagen surface was treated like the previous sample. Although several markers are present on the surface (white arrow), these nonspecifically bound particles do not form clusters and are, therefore, readily distinguishable from specifically bound gold. Collagen layer covers the surface uniformly and forms small filaments (black arrow). Pictures taken in tapping mode AFM have lateral dimensions of $5 \times 5 \mu\text{m}$ (for A and C) or $1 \times 1 \mu\text{m}$ (B), height scale ranges from 0 to 20 nm (bright to dark). Ultralever "D" tip, $F = 158 \text{ kHz}$, setpoint is approximately 90% of the free vibration amplitude.

not washed away even after 15 minutes of perfusion at 4.55 N/m² shear stress.

Morphology of VWF in function of shear stress

Independently of the applied shear stress, VWF adsorbed onto calf skin collagen-coated glass surfaces showed a roughly globular or irregular morphology (Figure 2), with no signs of the long, straight, uncoiled structure described earlier,⁶ and lack of any specific orientation, either parallel or perpendicular to the flow direction. Although it is difficult to perform precise lateral size measurements with AFM because of nonlinear tip convolution effects—the finite size tip does not always touch the surface features with its apex but often with its side; thus, apparent lateral dimension of scanned objects may become significantly larger than in reality—the most elongated clusters were always composed of at least 2 adjacent rows of gold beads. This observation suggests that width of the underlying VWF molecule should not be significantly thinner than 30 nm, considering the fact that gold beads have a diameter of at least 15 nm. This finding contrasts with those of Siedlecki et al⁶ who have imaged almost 1000-nm long but very thin, uncoiled forms of VWF. Our high shear regime used corresponds to approximately 4.55 N/m²; this value is significantly greater than the 3.5 N/m² reported as being the critical shear stress required to partially uncoil VWF. It is important to note, however, that some large, irregularly shaped VWF molecules were present near the coverslip edge for the high but not for the low shear regime (Figure 2F).

The results obtained from morphologic analysis of at least 4 distant fields of view (5 × 5 μm) taken from the flow area of either the low or the high shear coverslip are depicted in Table 1. (For sake of correctness, objects touching the image edges have been eliminated during morphologic analysis.) These observations could be repeated with another similar experiment (Table 1). The slight differences between the 2 sets of experiments are likely caused by differences in tip sharpness. In comparing the low and high shear stress regimes, no significant differences could be observed about the mean molecule size, mean particle roundness, mean eccentricity, mean feret diameter, or the mean major axis angle. High SD values for this latter indicate that molecules are almost randomly oriented in respect to the flow direction. A larger number of irregularly shaped molecules were found, however, at high shear stress. Finally, it can be clearly seen that the surface coverage after

5 minutes of VWF perfusion is almost 2-fold at high than at low shear. This observation, consistently with quantitative data on VWF binding to collagen at different shear conditions (J.H., L.N., J. Vermynen, and H.D., manuscript under preparation), can be explained by the fact that the flow chamber used for the high shear experiment has a narrower chamber slit and, additionally, should be used at a higher flow rate (25 mL/minute in contrast to 10 mL/minute for the low shear rate chamber) to attain the required wall shear stress value, thus a higher amount of VWF circulates over the coverslips shear area during a given perfusion time.

If roundness values of the VWF molecules are plotted against their area (Figure 3A-D), very similar “cloud plots” are obtained for the low and the high shear regimes. In the latter case, however, a few very large and quite irregularly shaped molecules could be seen (Figure 2F), which were completely absent from the low shear experiment.

To determine whether differences in surface coverage are caused by the differences in mass transfer rate, a series of experiments was performed with longer perfusion times to minimize adsorption time-based effects. After 15 minutes of perfusion, no significant differences in surface coverage were found (5.7% and 6.0% for 0.07 N/m² and 4.55 N/m² shear rate, respectively). All the morphologic factors studied are also identical within the measurement errors, according to the calculated SD values (Table 2), and, interestingly enough, the very large molecules observed at 4.55/m² but not at 0.07 N/m² during previous experiments with 5 minutes of perfusion are absent. These data further confirm the lack of significant differences between VWF morphology at the 2 shear regimes.

Shear-dependent morphology of VWF in the presence of fixed platelets

While studying shear-induced effects on VWF, it has to be kept in mind that under physiologic conditions, circulating platelets, leukocytes, and red blood cells are also present. These cellular elements have sizes and especially weights largely exceeding those of VWF molecules and, therefore, have higher momentum. It is possible that drifting platelets interacting momentarily with VWF multimers through their GPIb receptors would exert high forces onto these multimers, and these forces would be able to “pull” VWF and modify its morphology far easier than fluid shear stress alone. If this hypothesis was valid, it might be expected that perfusion in the presence of platelets should readily modify the

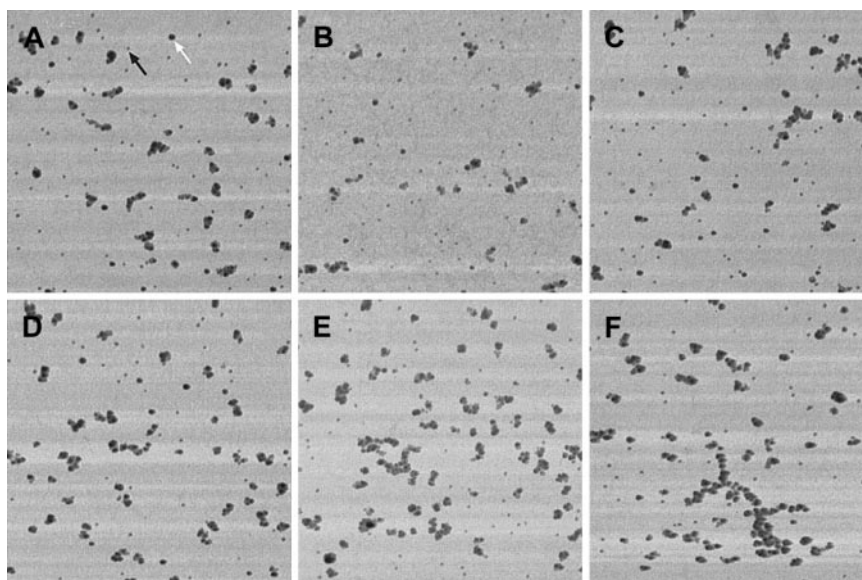


Figure 2. Shear-dependent morphology of VWF adsorbed onto collagen. PBS containing 1 μg/mL VWF was perfused at 0.07 N/m² (A-C) or at 4.55 N/m² (D-F) shear stress for 5 minutes over calf skin collagen-coated coverslips. No morphologic differences are apparent between the samples obtained at low or at high shear regimes. Double labeling with 15-nm and 30-nm gold-conjugated protein A (the black arrow points at a 15-nm gold bead, the white arrow shows a 30-nm gold particle). Tapping-mode AFM, Microlever “F” tip, F = 118 kHz, setpoint is approximately 90% of the free vibration amplitude. Image dimensions: 5 × 5-μm lateral and 40-nm height range.

Table 1. Morphologic properties of individual VWF molecules after 5 minutes of perfusion with 1 $\mu\text{g/mL}$ VWF over collagen as determined by image analysis of the digital pictures (mean \pm SD)

Shear stress	First experiment		Second experiment	
	0.07 N/m ²	4.55 N/m ²	0.07 N/m ²	4.55 N/m ²
Number of measured molecules	210	378	186	336
Surface coverage, %	4.06	7.92	4.94	8.04
Mean area, square pixels	253 \pm 180	330 \pm 434	279 \pm 152	314 \pm 440
Mean perimeter, pixels	71 \pm 38	79 \pm 60	74 \pm 27	87 \pm 88
Mean major axis length, pixels	22 \pm 11	25 \pm 14	24 \pm 8	27 \pm 16
Mean major axis angle, degrees	15 \pm 43	10 \pm 38	21 \pm 34	20 \pm 35
Mean minor axis length, pixels	14 \pm 5	15 \pm 9	15 \pm 5	15 \pm 8
Mean minor axis angle, degrees	-13 \pm 59	-13 \pm 63	-28 \pm 59	-25 \pm 58
Mean eccentricity	1.67 \pm 0.58	1.62 \pm 0.42	1.77 \pm 0.59	1.83 \pm 0.55
Mean roundness	0.66 \pm 0.20	0.67 \pm 0.19	0.64 \pm 0.14	0.58 \pm 0.17
Mean feret diameter, pixels	17 \pm 6	19 \pm 9	18 \pm 5	19 \pm 8

As all morphologic measures are performed on digitalized images, dimensions are given in pixels instead of nanometers. Theoretically on a $5 \times 5\text{-}\mu\text{m}$ image sampled at 512 pixels per line and 512 pixels per row, one pixel corresponds to approximately 9.77 nm (real dimensions are, however, somewhat different because of tip spatial convolution effects).

morphology of individual VWF molecules at high compared with low shear stress.

Therefore, we performed a 15-minute perfusion in the presence of 1 μg VWF and $68 \times 10^6/\text{mL}$ washed, formal-fixed platelets.

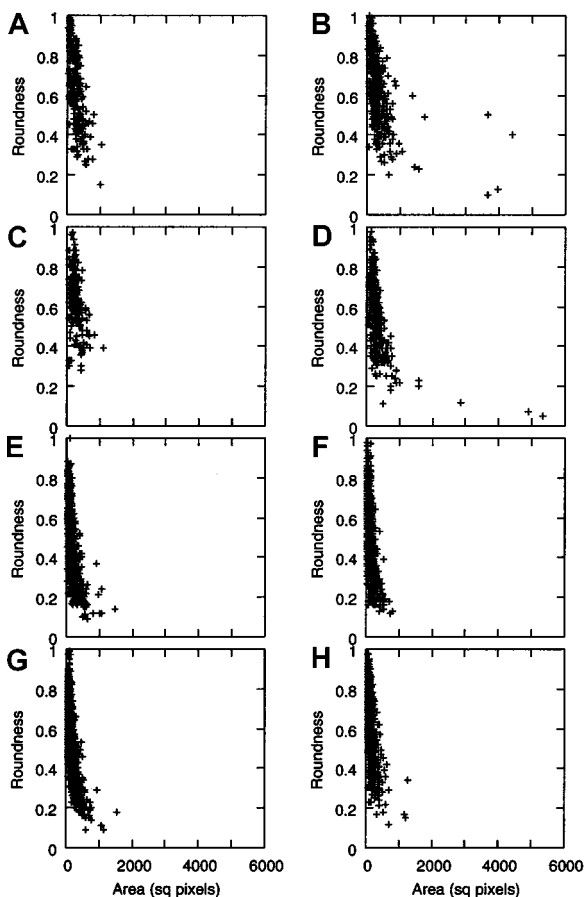


Figure 3. Roundness versus area plot of VWF molecules in function of shear stress. The stacked graphs representing data from 4 experiments are shown (A,C,E,G: low shear; B,D,F,H: high shear). After 5 minutes of VWF perfusion over collagen surface, size distribution of gold bead-covered area is similar at low (A, 1st experiment; C, 2nd experiment) and at high shear (B, 1st experiment; D, 2nd experiment), but some very large molecules are present only in the latter case (points at the right side of B and D). Cloud plots for the roundness versus area graphs show that irregularity of VWF molecules seems to correlate with their area size, and highly irregular molecules are also unusually large. When perfusing for 15 minutes, such large molecules could not be detected anymore, neither in the absence (E-F) nor in the presence (G-H) of fixed platelets in the perfusate. AFM parameters are identical to those in Figure 1.

Without fixation, platelets would adhere to the collagen layer through their GPIb-IIa and/or GPVI receptors or make permanent bonds with VWF by the GPIIb-IIIa integrins. GPIb alone does not seem to support firm adhesion of platelets to VWF; instead, cells expressing only this receptor roll on the surface, whereas bonds permanently make up and break.^{5,11}

The low platelet count used does not significantly alter the viscosity of the perfusate. Before the perfusion, functionality of platelets was checked with the ristocetin-dependent platelet agglutination test. The fixed platelets mixed with 1 $\mu\text{g/mL}$ VWF in PBS slowly aggregated into small aggregates on the addition of ristocetin (final concentration of 1.5 mg/mL), meaning that GPIb receptors were at least partly active. No platelets were adhering to the collagen, indicating that collagen receptors are no longer active because of the fixation.

On perfusion, the measured morphologic parameters, listed in Table 3, did not indicate any shape change of VWF at 6500/s shear rate compared with that at 100/s (because of the presence of platelets, fluid viscosity; thus, shear stress values are somewhat higher in these cases than in PBS containing 1 $\mu\text{g/mL}$ VWF only). Additionally, the surface coverage by VWF was higher at low than at high shear stress, which is opposite of what was found for the two 5-minute perfusion experiments. This observation is further confirmed by the roundness-area plots (Figure 3G,H).

Discussion

We have studied the morphology of VWF bound to immobilized calf skin type I collagen under shear stress of 0.07 N/m² (low shear)

Table 2. Morphologic properties of individual VWF molecules (mean \pm SD) after 15 minutes of perfusion of collagen-coated coverslips with 1 $\mu\text{g/mL}$ VWF

Shear stress	0.07 N/m ²	4.55 N/m ²
Number of measured molecules	599	896
Surface coverage, %	5.7	6.0
Mean area, square pixels	182 \pm 149	128 \pm 93
Mean perimeter, pixels	74 \pm 45	59 \pm 32
Mean major axis length, pixels	20 \pm 10	17 \pm 7
Mean major axis angle, degrees	-4 \pm 43	7 \pm 42
Mean minor axis length, pixels	12 \pm 5	10 \pm 4
Mean minor axis angle, degrees	13 \pm 61	3 \pm 63
Mean eccentricity	1.80 \pm 0.6	1.80 \pm 1.2
Mean roundness	0.48 \pm 0.18	0.50 \pm 0.17
Mean feret diameter, pixels	14 \pm 5	12 \pm 4

Table 3. Morphologic properties of individual VWF molecules (mean \pm SD) after 15 minutes of perfusion with 1 μ g/mL VWF and 68 $\times 10^9$ /L fixed washed platelets

Shear stress	> 0.07 N/m ²	> 4.55 N/m ²
Number of measured molecules	795	534
Surface coverage, %	7.8	4.5
Mean area, square pixels	180 \pm 143	177 \pm 130
Mean perimeter, pixels	67 \pm 42	63 \pm 32
Mean major axis length, pixels	20 \pm 9	19 \pm 8
Mean major axis angle, degrees	-10 \pm 40	-1 \pm 39
Mean minor axis length, pixels	12 \pm 5	12 \pm 5
Mean minor axis angle, degrees	5 \pm 62	3 \pm 64
Mean eccentricity	1.72 \pm 0.48	1.72 \pm 0.50
Mean roundness	0.56 \pm 0.18	0.60 \pm 0.17
Mean feret diameter, pixels	14 \pm 5	14 \pm 4

and 4.55 N/m² (high shear), using parallel-plate perfusion chambers and AFM.

The major difficulty in morphology experiments performed on VWF bound to collagen surface with AFM resides in the uneven topography of the collagen layer, making it difficult if not impossible to differentiate collagen from bound VWF by direct topographic measurements. This difficulty can be overcome by immunogold labeling of VWF, as carefully chosen size gold markers can be unequivocally identified by AFM, whereas they have enough lateral resolution for quantitative work, even on corrugated surfaces like whole cells.¹²⁻¹⁵ Immunogold was already successfully applied to label VWF either for electron microscopy,^{16,17} or for AFM.¹⁰ In our case, a specific immunogold procedure had to be elaborated that permits high-efficiency labeling with acceptable level of nonspecific background.

As the effect of VWF on platelet arrest, in contrast to fibrinogen, becomes significant only at high shear rates,¹ it is widely considered that this phenomenon would be due to a shear stress-induced morphologic or conformational change of the VWF molecule. (We think it is important to dissociate between morphologic and conformational changes, because the former refers to the shape of the multimeric molecule, whereas the term "conformational change" suggests a modification of the three-dimensional arrangement of its amino-acid backbone on a much smaller scale.) It is known from previous studies that some VWF fragments in which the A1 domain is altered show either an increased or a reduced binding to GPIIb.^{18,19} VWF can undergo a shape change in certain conditions: when heated to 55°C, VWF unfolds and stretches, with no apparent loss of antigenicity and of the multimerization degree of the molecule.¹⁷ This form is thought to possess increased ability to support platelet adhesion. Moreover, different (globular and linear) morphologic forms of VWF could be visualized either with electron microscopy² or with AFM.⁶ In the latter case, VWF was subjected to a shear force gradient in a cone-and-plate rotating device, and the authors demonstrated the existence of long, uncoiled molecules among the preponderant globular forms when shear stress exceeded a threshold limit of 3.5 N/m². This experiment seems to sustain the hypothesis of shear-induced modifications in the three-dimensional structure of VWF, but the substrate used was artificial (octadecyl-trichlorosilane self-assembling monolayer on glass, developed to provide an optimally flat surface for direct observation of protein molecules) and does not necessarily have the same properties toward VWF as its natural binding substrates, the adhesive proteins found in subendothelial matrices, like collagens. Additionally, it seems that the molecule shape itself can also depend on the surface properties.²⁰

Our data do not confirm shear-induced morphologic change of VWF. Although the high shear stress used was clearly larger than

the threshold value during the experiments of Siedlecki et al⁶ (4.55 N/m² versus 3.5 N/m²), no significant differences were found in respect to all studied mean morphologic parameters. Unfolding of the molecules would result in an increase of the mean eccentricity and decrease of mean roundness or both. Additionally, it is expected that a molecule becoming filamentous under shear stress would orient itself in the direction of the shear, that is parallel to the flow in our experimental setup. Again, no such observation could be made.

These considerations are based on the assumption that fluid shear force alone is sufficient to "pull" VWF molecules into an elongated morphology. It is not impossible that even if a physiologic shear stress is unable to cause such changes, the interaction with a drifting platelet (having a relatively high momentum) could exert enough force to uncoil the molecule. We did not find such effect when using fixed washed platelets, but this does not constitute a solid proof by itself, as the fixation alters the flexibility of the platelets and also inactivates several cell surface receptors that might be required for this interaction to occur.

The possibility remains of VWF "recoiling" into its nonactive morphology when the shear stress ceases. To avoid this effect, the first 3 minutes of fixation were always performed in the presence of shear. Past this time, it is unlikely that the protein stabilized by crosslinks would be able to recoil. Additionally, the shear-dependent morphology change of VWF described earlier was observed out of flow, about 5 minutes after the coverslip being dismantled from the shearing device.⁶

However, larger VWF multimers are more active in promoting platelet adhesion,⁹ and some unusually large molecules were present at the high shear regime, when perfusion was performed for 5 minutes. These molecules had also a fairly lobulated shape, which could be consistent with shear-induced morphologic changes. It is important to note, however, that (1) all VWF molecules tend to become more lobulated with increasing surface area as shown by Figure 3, independently of the shear regime; (2) we do not know whether these irregular large molecules were unwound while binding to the surface, or they already had a less compact shape in solution; (3) the area occupied by the largest multimers is still small compared with the total VWF-covered area; and, finally, (4) these large molecules lack any specific orientation toward the flow direction, like the smaller ones. Additionally, such large molecules were not found when the perfusion time was increased to 15 minutes. We do not know whether this latter phenomenon is due to a shear-mediated detachment of VWF. Previous observations indicated that platelets already attached to a surface can detach from it under the influence of shear forces, especially if they did not yet undergo a shape change.²¹ Effectively, the largest VWF multimers were preferentially found downstream. Although there is no direct proof sustaining the following hypothesis, it is not impossible that, under influence of shear forces, these VWF molecules would translocate on collagen. In this way, although VWF is perfused over the surface, larger multimers would progress by slow motion in the flow direction. When VWF solution is substituted by PBS and then paraformaldehyde, this translocation would continue further until cross-linking to the matrix through formaldehyde-induced bonds would definitively fix the molecules. During the time needed for this cross-linking to occur, multimers near the outlet could escape, whereas those upward would have moved in the direction of the coverslip's back edge. Even if it is usually considered that larger molecules bind more efficiently to the surface than smaller ones because of their multiple anchoring sites, a not-fully-attached large molecule, which has side arms well apart from the surface, could be more prone to shear-induced

detachment. This hypothesis does not contradict the observations made by previous researchers on a silanized surface: Binding of VWF to this latter type of matrix is strong,⁶ apparently stronger than to calf skin collagen, shown by the fact that 5 minutes of perfusion with buffer containing only 50 ng/mL VWF produces a relatively high surface coverage on octadecyl-trichlorosilane; whereas on calf skin collagen, we have never obtained coverage of more than 10% of the surface, even at 1 $\mu\text{g/mL}$ VWF.

Our observations do not seem to sustain the significance of shear-induced VWF shape modifications. This observation does not rule out that shear actually has a strong influence on VWF–GPIb interaction. Certain gain-of-function mutations of the VWF A1 domain can alter its conformation,²² and this change might explain the increased avidity of the modified VWF domain toward GPIb. Although the shear-dependency of platelet tethering on these fragments was reduced as their static GPIb-binding capacity increased, it is not impossible that shear forces could be at the origin of a similar conformational change. In all cases, the scale of these events is clearly smaller than that of the resolution of actual AFM techniques. However, an enhanced binding of VWF to recombinant GPIb α chains when GPIb glycine 223 is mutated to valine was also observed.²³ One, therefore, cannot rule out the possibility that shear forces could act even on GPIb.

The data obtained during our experiments tend to favor the hypothesis of a constitutive, fast on-off rate interaction between VWF and GPIb^{22,24} and not that of a shear-induced morphology-dependent affinity increase toward GPIb. At least, no major

differences were found in the overall morphology of individual VWF molecules exposed to high in comparison to low shear. In addition, the probability of VWF “recoiling” past the perfusion was kept small by performing the washing and part of the fixation in flow. Although it is by no means definitive proof, it seems unlikely that the generally large shear-dependent differences of VWF’s effect onto platelet tethering could be explained by the presence of some rare irregular and larger multimers found during 5 minutes of perfusion time experiments (additionally, these larger multimers were absent when perfusing for 15 minutes).

In conclusion, our experiments did not show a significant overall morphologic shape change of VWF molecules bound to collagen under high shear, even if some large, irregular molecules were observed in certain conditions. This does not exclude a possible effect of shear on one or more domain(s) of VWF, but such small-scale changes cannot be studied by conventional AFM techniques. Our findings further support the hypothesis of a constitutive interaction between VWF A1 domain and platelet GPIb.

Acknowledgments

We thank Andrea Sümegi for the PAGE-SDS of VWF under reducing conditions, and Drs Tamás Bistey, Péter Nagy, György Vámosi, and Attila Jenei for their help concerning atomic force microscopic measures.

References

- Ruggeri ZM, Saldívar E. Platelets, hemostasis and thrombosis. In: Ruggeri ZM, ed. *von Willebrand Factor and the Mechanisms of Platelet Function*. Berlin, Germany: Springer; 1998:1-32.
- Fowler WE, Fretto LJ, Hamilton KK, Erickson HP, McKee PA. Substructure of human von Willebrand factor. *J Clin Invest*. 1985;76:1491-1500.
- Savage B, Saldívar E, Ruggeri ZM. Initiation of platelet adhesion by arrest onto fibrinogen or translocation on von Willebrand factor. *Cell*. 1996;84:289-297.
- Moake JL, Turner NA, Stathopoulos NA, Nolasco LH, Hellums JD. Involvement of large plasma von Willebrand factor (vWF) multimers and unusually large vWF forms derived from endothelial cells in shear stress-induced platelet aggregation. *J Clin Invest*. 1986;78:1456-1461.
- Fredrickson BJ, Dong J-F, McIntire LV, López JA. Shear-dependent rolling on von Willebrand factor of mammalian cells expressing the platelet glycoprotein Ib-IX-V complex. *Blood*. 1998;92:3684-3693.
- Siedlecki CHA, Lestini BJ, Kottke-Marchant K, Eppell SJ, Wilson DL, Marchant RE. Shear-dependent changes in the three-dimensional structure of human von Willebrand factor. *Blood*. 1996;88:2939-2950.
- Horisberger M, Rosset J. Colloidal gold, a useful marker for transmission and scanning electron microscopy. *J Histochem Cytochem*. 1977;25:295-305.
- Sakariassen KS, Aarts PAMM, de Groot PG, Houdijk WPM, Sixma JJ. A perfusion chamber developed to investigate platelet interaction in flowing blood with human vessel wall cells, their extracellular matrix, and purified components. *J Lab Clin Med*. 1983;102:522-535.
- Wu Y-P, van Breugel HHFI, Lankhof H, et al. Platelet adhesion to multimeric and dimeric von Willebrand factor and to collagen type III preincubated with von Willebrand factor. *Arterioscler Thromb Vasc Biol*. 1996;16:611-620.
- Raghavachari M, Kottke-Marchant K, Marchant RE. Determining intramolecular binding sites on surface-bound von Willebrand factor under aqueous conditions. *Thromb Res*. 2000;98:351-358.
- Cranmer SL, Ulsemer PH, Cooke BM, et al. Glycoprotein (GP) Ib-IX-transfected cells roll on a von Willebrand matrix under flow. *J Biol Chem*. 1999;274:6097-6106.
- Eppell SJ, Simmons SR, Albrecht RM, Marchant RE. Cell-surface receptors and proteins on platelet membranes imaged by scanning force microscopy using immunogold contrast enhancement. *Biophys J*. 1995;68:671-680.
- Damjanovich S, Vereb Gy, Schaper A, et al. Structural hierarchy in the clustering of HLA class I molecules in the plasma membrane of human lymphoblastoid cells. *Proc Natl Acad Sci U S A*. 1995;92:1122-1126.
- Damjanovich S, Gáspár R, Pieri C. Dynamic receptor superstructures at the plasma membrane. *Q Rev Biophys*. 1997;30:67-106.
- Jenei A, Varga S, Bene L, et al. HLA class I and II antigens are partially co-clustered in the plasma membrane of human lymphoblastoid cells. *Proc Natl Acad Sci U S A*. 1997;94:7269-7274.
- Furlan M, Robles R, Lämmle B, Zimmermann J, Hunziker E. Immunogold labelling of human von Willebrand factor adsorbed to collagen. *Blood Coagul Fibrinol*. 1991;2:441-446.
- Post MJ, de Graaf-Bos AN, Posthuma G, de Groot PG, Sixma JJ, Borst C. Interventional thermal injury of the arterial wall: unfolding of Willebrand factor and its increased binding to collagen after 55°C heating. *Thromb Haemost*. 1996;75:515-519.
- Miyata S, Goto S, Federici AB, Ware J, Ruggeri ZM. Conformational changes in the A1 domain of von Willebrand factor modulating the interaction with platelet glycoprotein Ib α . *J Biol Chem*. 1996;271:9046-9053.
- Lankhof H, Damas C, Schiphorst ME, et al. Functional studies on platelet adhesion with recombinant von Willebrand factor type 2B mutants R543Q and R543W under conditions of flow. *Blood*. 1997;89:2766-2772.
- Raghavachari M, Tsai H, Kottke-Marchant K, Marchant RE. Surface dependent structures of von Willebrand factor observed by AFM under aqueous conditions. *Colloids Surf B Biointerfaces*. 2000;19:315-324.
- Wu Y-P, de Groot PG, Sixma JJ. Shear stress-induced detachment of blood platelets from various surfaces. *Arterioscler Thromb Vasc Biol*. 1997;17:3202-3207.
- Miyata S, Ruggeri ZM. Distinct structural attributes regulating von Willebrand factor A1 domain interaction with platelet glycoprotein Ib α under flow. *J Biol Chem*. 1999;274:6586-6593.
- Marchese P, Saldívar E, Ware J, Ruggeri ZM. Adhesive properties of the isolated amino-terminal domain of platelet glycoprotein Ib α in a flow field. *Proc Natl Acad Sci U S A*. 1999;96:7837-7842.
- Savage B, Almus-Jacobs F, Ruggeri ZM. Specific synergy of multiple substrate-receptor interactions in platelet thrombus formation under flow. *Cell*. 1998;94:657-666.